1521-0111/90/3/205–213$25.00
MOLECULAR PHARMACOLOGY

http://dx.doi.org/10.1124/mol.116.104133
Mol Pharmacol 90:205–213, September 2016

Involvement of Spinal Angiotensin II System in Streptozotocin-Induced Diabetic Neuropathic Pain in Mice

Yoshiki Ogata, Wataru Nemoto, Osamu Nakagawasai, Ryota Yamagata, Takeshi Tadano, and Koichi Tan-No

Department of Pharmacology, Faculty of Pharmaceutical Sciences, Tohoku Medical and Pharmaceutical University, Aoba-ku, Sendai, Japan (Y.O., W.N., O.N., R.Y., K.T.-N.); Department of Health Care Medical Research, Venture Business Laboratory, Kanazawa University, Kanazawa, Japan (T.T.)

Received March 1, 2016; accepted July 6, 2016

ABSTRACT

Renin-angiotensin system (RAS) activity increases under hyperglycemic states, and is thought to be involved in diabetic complications. We previously demonstrated that angiotensin (Ang) II, a main bioactive component of the RAS, might act as a neurotransmitter and/or neuromodulator in the transmission of nociceptive information in the spinal cord. Here, we examined whether the spinal Ang II system is responsible for diabetic neuropathic pain induced by streptozotocin (STZ). Tactile allodynia was observed concurrently with an increase in blood glucose levels the day after mice received STZ (200 mg/kg, i.v.) injections. Tactile allodynia on day 14 was dose-dependently inhibited by intrathecal administration of losartan, an Ang II type 1 (AT1) receptor antagonist, but not by PD123319, an AT2 receptor antagonist. In the lumbar dorsal spinal cord, the expression of Ang II, Ang converting enzyme (ACE), and phospho-p38 mitogen-activated protein kinase (MAPK) were all significantly increased on day 14 after STZ injection compared with vehicle-treated controls, whereas no differences were observed among AT1 receptors or angiotensinogen levels. Moreover, the increase in phospho-p38 MAPK was significantly inhibited by intrathecal administration of losartan. These results indicate that the expression of spinal ACE increased in STZ-induced diabetic mice, which in turn led to an increase in Ang II levels and tactile allodynia. This increase in spinal Ang II was accompanied by the phosphorylation of p38 MAPK, which was shown to be mediated by AT1 receptors.

Introduction

The renin angiotensin (Ang) system (RAS) is involved in regulating blood pressure and fluid and electrolyte homeostasis (Kobori et al., 2007). In the RAS, angiotensinogen (AGT) is metabolized into Ang I, and Ang I is then converted to Ang II by Ang converting enzyme (ACE) (Paul et al., 2006; Campbell, 2014). The evidence indicates that Ang II, a main bioactive component of the RAS, affects a wide range of central and peripheral components of the sensory systems (Wu et al., 2000; Burkhalter et al., 2001; Pelegrini-da-Silva et al., 2005), and is mediated by Ang II type 1 (AT1) and Ang II type 2 (AT2) receptors.

Traditionally, Ang II has been considered to be generated by the circulating RAS, but additional local organ-specific RASs have been confirmed to exist in several organs (Bader, 2010). In both rat and human dorsal root ganglia (DRGs) Ang II is colocalized in two known regulators for nociception and sensory transmission: substance P and calcitonin gene–related peptide (Patil et al., 2010). We have previously demonstrated that when mice are administered Ang II intrathecally, p38 mitogen-activated protein kinase (MAPK) is phosphorylated through AT1 receptors, leading to nociceptive behavior (Nemoto et al., 2013, 2015a). Moreover, injections of 2% formalin into mice hind paws increases Ang II approximately 1.5-fold on the ipsilateral side of the lumbar superficial dorsal horn, and AT1 receptor antagonist losartan dose-dependently produces an antinociceptive effect by inhibiting p38 MAPK phosphorylation (Nemoto et al., 2015b). Taken together, Ang II may act as a neurotransmitter and/or neuromodulator in the spinal transmission of nociceptive information.

Neuropathy occurs in about 50% of patients with diabetes (Dyck et al., 1993; Veves et al., 2008) as a diffuse symmetric injury to peripheral nerves, and has major implications on the quality-of-life and public health costs (Gordois et al., 2003;

This study was supported in part by the Japan Society for the Promotion of Science [KAKENHI Grants 26460101 and 16K21311]; and a Matching Fund Subsidy for Private Universities from the Ministry of Education, Culture, Sports, Science and Technology of Japan [Grant S1511001L].

Y.O. and W.N. contributed equally to this study.

dx.doi.org/10.1124/mol.116.104133.

ABBREVIATIONS: ACE, Ang-converting enzyme; AGT, angiotensinogen; Ang, angiotensin; ANOVA, analysis of variance; AT1, angiotensin II type 1; AT2, angiotensin II type 2; bp, base pair; DRG, dorsal root ganglion; ECL, enhanced chemiluminescence; GAPDH, glyceraldehyde-3-phosphate dehydrogenase; GFAP, glial fibrillary acidic protein; Iba-1, ionized calcium binding adaptor molecule 1; IR, immunoreactive; MAPK, mitogen-activated protein kinase; NDS, normal donkey serum; NeuN, neuronal nuclei; NGS, normal goat serum; PBS, phosphate-buffered saline; PD123319, 1-[[4-(dimethylamino)-3-methylphenyl]methyl]-5-(diphenylacetyl)-4,5,6,7-tetrahydro-1H-imidazo[4,5-c]pyridine-6-carboxylic acid ditrifluoroacetate; RAS, renin-angiotensin system; RT-PCR, reverse-transcription polymerase chain reaction; STZ, streptozotocin; TBST, Tris-buffered saline supplemented with 0.01% Tween-20.

Boulton et al., 2005). One of the prominent pathognomonic symptoms of diabetic neuropathy is neuropathic pain, which affects 16% of patients with diabetes, but is frequently unreported (12.5%) and often inadequately treated (39%) (Daousi et al., 2004). The pathogenesis of diabetic neuropathic pain is complex and thus remains poorly understood.

In the diabetic state, there is an increase in plasma ACE activity and levels of Ang II (Van Dyk et al., 1994; van Dijk et al., 2001) and there have been many studies conducted on the relationship between RAS and diabetic complications. One of the outcomes of RAS activation is the hypertrophy of various renal cells promoted by Ang II, which leads to the development of diabetic nephropathy (Leehey et al., 2000; Vidotti et al., 2004). Evidence obtained from both animal and clinical studies supports the hypothesis that nephropathy can be effectively treated by intrarenal RAS blockade (Hollenberg et al., 2003). In addition, the retinal RAS is also activated in diabetic mice and treatment with AT1 receptor antagonists significantly ameliorates the course of retinopathy (Ebrahimian et al., 2005). Although the role of spinal RAS on diabetic neuropathic pain has not been studied to date, these reports suggest that RAS is also activated in the spinal cord and is involved in diabetic neuropathic pain.

Thus, in the present study we examined whether the spinal RAS is responsible for diabetic neuropathic pain using the streptozotocin (STZ)-induced diabetic mouse model.

Materials and Methods

Animals

Male ddY mice (26–30 g; Japan SLC Inc., Hamamatsu, Japan) were housed in cages with food and water provided ad libitum under constant temperature (22 ± 2°C) and humidity (55 ± 5%), with a 12-hour light/dark cycle (lights on: 8:00 AM to 8:00 PM). Mice were separated into groups of 10–20 mice for behavioral experiments, 5–6 for reverse-transcription polymerase chain reaction (RT-PCR), 4–6 for Western blotting, and 4–10 for immunohistochemical experiments in single experiments. The Ethics Committee of Animal Experiments at Tohoku Medical and Pharmaceutical University approved all experiments according to the National Institutes of Health Guide for the Care and Use of Laboratory Animals (https://grants.nih.gov/grants/olaw/Guide-for-the-Care-and-use-of-laboratory-animals.pdf). Efforts were made to minimize suffering and to reduce the number of animals used.

Induction of Diabetes

STZ (Sigma-Aldrich, St. Louis, MO) was dissolved in 0.1 N citrate buffer (pH 4.5), and a single intravenous injection was given to mice promptly thereafter to induce diabetes (Kamei et al., 1991). Control mice were injected with vehicle alone. Blood samples from the tail vein were taken to measure blood glucose levels via the FreeStyle Optium Blood Glucose Monitoring System (Abbott Japan Co. Ltd., Osaka, Japan).

Intrathecal Injections

Intrathecal injections were performed as previously described (Nemoto et al., 2013, 2014, 2015a,b).

Behavioral Studies

Tactile allodynia was determined by assessing paw withdrawal via the von Frey filament test. Mice were placed on a mesh floor inside a clear plastic cubicle and were allowed to acclimatize for at least 30 minutes before the tests. Thereafter, von Frey filaments (pressure applied by each filament: 0.07, 0.16, 0.4, 0.6, 1.0, and 1.4 g) were applied perpendicularly against the plantar surface of the left and right hind paws from beneath the mesh floor and held for 3 seconds with slight buckling of the filaments. If the paw was sharply withdrawn, a positive response was recorded, and the next weakest von Frey hair was applied. On the other hand, if a negative response occurred, the next strongest force was applied. The mean left and right paw scores of trials for each mouse were calculated.

Stimulation of equal intensity (0.4-g filament) was applied to the plantar surface of the left and right hind paws, and repeated 10 times at intervals of 5 seconds to assess the dose-dependent effect of losartan on tactile allodynia. The frequency of sharp withdrawal responses was measured.

Drugs and Antibodies

The following drugs and reagents were used: losartan potassium (LKT Laboratories, St Paul, MN); 1-[[4-(dimethylamino)-3-methylphenyl]methyl]-5-(diphenylacetyl)-4,5,6,7-tetrahydro-1H-imidazo[4,5-c]pyridine-6-carboxylic acid ditrifluoroacetate (PD123319; Tocris Bioscience, Ellisville, MO); sodium pentobarbital (Kyoritsu Seiyaku

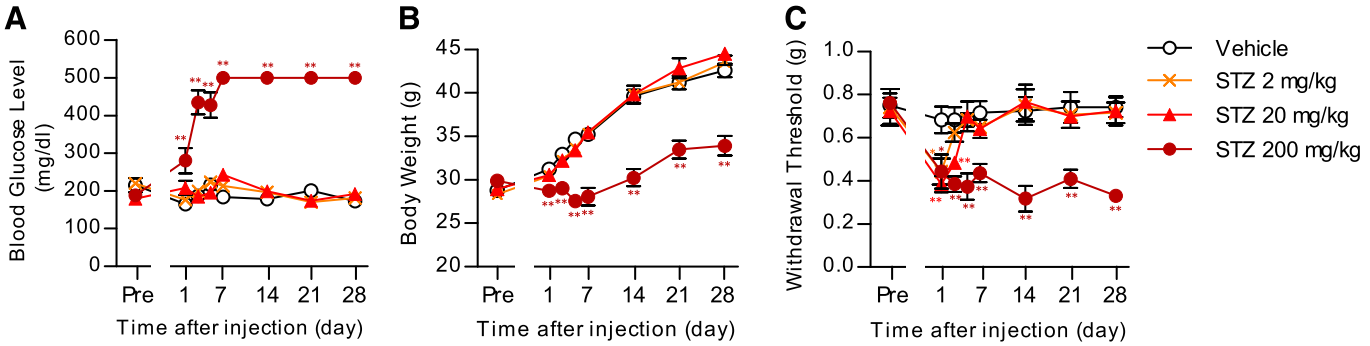

Fig. 1. Changes in blood glucose levels, body weights, and tactile allodynia in STZ mice. Blood glucose levels (A), body weights (B), and tactile allodynia (C) were monitored over 28 days after the injection of STZ (2-200 mg/kg, i.v.). (A) Two-way ANOVA: group ($F_{3,22} = 200.97$, $P < 0.01$); time ($F_{7,154} = 16.78$, $P < 0.01$); group × time ($F_{21,154} = 20.77$, $P < 0.01$). One-way ANOVA: before (pre), $F_{3,22} = 2.08$, $P = 0.13$; day 1, $F_{3,22} = 5.39$, $P < 0.01$; day 3, $F_{3,22} = 34.13$, $P < 0.01$; day 5, $F_{3,22} = 23.47$, $P < 0.01$; day 7, $F_{3,22} = 224.93$, $P < 0.01$; day 14, $F_{3,22} = 420.87$, $P < 0.01$, day 21, $F_{3,22} = 1002.69$, $P < 0.01$, day 28, $F_{3,22} = 583.84$, $P < 0.01$. (B) Two-way ANOVA: group ($F_{3,22} = 57.78$, $P < 0.01$); time ($F_{7,154} = 207.84$, $P < 0.01$); group × time ($F_{21,154} = 18.85$, $P < 0.01$). One-way ANOVA: pre, $F_{3,22} = 3.12$, $P < 0.05$; day 1, $F_{3,22} = 9.08$, $P < 0.01$; day 3, $F_{3,22} = 16.94$, $P < 0.01$; day 5, $F_{3,22} = 34.91$, $P < 0.01$; day 7, $F_{3,22} = 26.32$, $P < 0.01$; day 14, $F_{3,22} = 31.79$, $P < 0.01$; day 21, $F_{3,22} = 24.09$, $P < 0.01$; day 28, $F_{3,22} = 26.32$, $P < 0.01$. (C) Two-way ANOVA: group ($F_{3,22} = 24.06$, $P < 0.01$); time ($F_{7,154} = 8.65$, $P < 0.01$); group × time ($F_{21,154} = 3.69$, $P < 0.01$). One-way ANOVA: pre, $F_{3,22} = 0.08$, $P = 0.97$; day 1, $F_{3,22} = 3.85$, $P < 0.05$; day 3, $F_{3,22} = 10.76$, $P < 0.01$; day 5, $F_{3,22} = 9.56$, $P < 0.01$; day 7, $F_{3,22} = 8.47$, $P < 0.01$; day 14, $F_{3,22} = 11.10$, $P < 0.01$; day 21, $F_{3,22} = 10.05$, $P < 0.01$; day 28, $F_{3,22} = 20.45$, $P < 0.01$. Values represent the mean ± S.E.M. for groups of 7–8 mice. *$P < 0.05$, **$P < 0.01$ compared with vehicle (0.1 N citrate buffer) controls.

Co., Tokyo, Japan); normal goat serum (NGS) (Invitrogen, Carlsbad, CA); normal donkey serum (NDS) (Rockland Immunochemicals Inc., Pottstown, PA); antibodies against p38 MAPK, phospho-p38 MAPK, and horseradish peroxidase–conjugated goat anti-rabbit IgG antibody (Cell Signaling Technology, Danvers, MA); rabbit anti-Ang II antibody (Phoenix Pharmaceuticals, Burlingame CA); rabbit anti-AT1 receptor antibody (Alpha Diagnostic International, San Antonio, TX); rabbit anti-ACE antibody, goat anti-ACE antibody (Santa Cruz Biotechnology, Dallas, TX); rabbit anti-AGT antibody (Proteintech, Chicago, IL); fluorescein isothiocyanate–labeled anti-rabbit IgG goat antiserum, mouse anti–glial fibrillary acidic protein (GFAP), and anti–neuronal nuclei (NeuN) antibodies (Millipore, Billerica MA); rabbit anti–ionized calcium binding adaptor molecule 1 (Iba-1) antibody (Wako Chemicals, Osaka, Japan); TRI Reagent (Sigma-Aldrich); ReverTraAce (Toyobo, Osaka, Japan); Go Taq quantitative PCR Master mix (Promega, Madison, WI); enhanced chemiluminescence (ECL) assay kit (GE Healthcare, Amersham, UK); and Alexa Fluor 488–conjugated goat anti-mouse IgG, Alexa Fluor 568–conjugated goat anti-rabbit IgG, Alexa Fluor 488–conjugated donkey anti-rabbit IgG, and Alexa Fluor 568–conjugated donkey anti-goat IgG (Molecular Probes, Eugene, OR). The antibody against ACE was used at a dilution of 1:50 for confocal microscopy, whereas other primary and secondary antibodies were diluted at 1:200. Losartan was dissolved in Ringer's solution (Fuso Pharmaceutical Industries, Osaka, Japan), and PD123319 was dissolved in Ringer's solution containing 6.8% dimethylsulfoxide (Wako Chemicals) for intrathecal injections.

Immunohistochemical Study

MapAnalyzer. Immunohistochemical staining was conducted as previously described (Nakagawasai et al., 2003; Nemoto et al., 2013, 2014, 2015b). The quantities of Ang II, phospho-p38 MAPK, ACE, AT1 receptors, or AGT in spinal cords [lumbar 5 (L5)] were determined as follows: 20-μm-thick slices were incubated overnight at 4°C with rabbit anti-Ang II antibody (diluted 1:50 with PBS containing 0.3% Triton X-100 and 1% NGS), rabbit anti-phospho-p38 MAPK antibody (1:100 dilution with PBS containing 1% NGS and 0.3% Triton X-100), rabbit anti-ACE antibody (1:50 dilution with PBS containing 1% NGS), rabbit anti-AT1 receptor antibody (1:100 dilution with PBS containing 1% NGS), or rabbit anti-AGT antibody (1:25 dilution with PBS containing 1% NGS and 0.3% Triton X-100), respectively. Slices were washed four times with PBS for 1.5 hours and incubated overnight at 4°C with fluorescein isothiocyanate–labeled anti-rabbit IgG goat antiserum (1:200 dilution with PBS containing 0.3% Triton X-100 and 1% NGS to determine the quantities of Ang II, AGT, and phospho-p38 MAPK, or 1% NGS only to determine ACE and AT1 receptors). The fluorescence intensity for Ang II, ACE, AT1 receptor, or AGT in both sides of the superficial dorsal horn (laminae I and II) 14 days after intravenous injection of vehicle was quantitated and set as 1.

Confocal Microscopy. Immunohistochemical staining was conducted as previously described (Nemoto et al., 2014, 2015a). Immunofluorescence double labeling was achieved by incubating 40-μm-thick slices with the primary antibodies, rabbit anti-ACE antibody, goat anti-ACE antibody, mouse anti-GFAP antibody, mouse anti-NeuN antibody, and/or rabbit anti-Iba-1 antibody, diluted with PBS containing 0.3% Triton-X and 1% NGS or NDS, correspondingly, overnight at 4°C. The secondary antibodies (diluted 1:200 with PBS containing 0.3% Triton-X and 1% NGS or NDS, respectively) reacted for 2 hours in the dark at room temperature. Fluorescence intensity was visualized on a D-Eclipse C1 microscope (Nikon, Kanagawa, Japan).

Western Blotting

Western blotting was conducted as previously described (Nemoto et al., 2013, 2014, 2015a). Electrophoresis was performed in 7.5% acrylamide gels for the detection of ACE; 10% acrylamide gels were used in all other cases. Proteins were transferred electrically from the gel onto a polyvinylidene difluoride membrane using a semi-dry blotting apparatus (Bio-Rad Laboratories, Tokyo, Japan). Blots were blocked with 5% skim milk in Tris-buffered saline (TBST) supplemented with 0.01% Tween-20 for 30 minutes, and incubated with

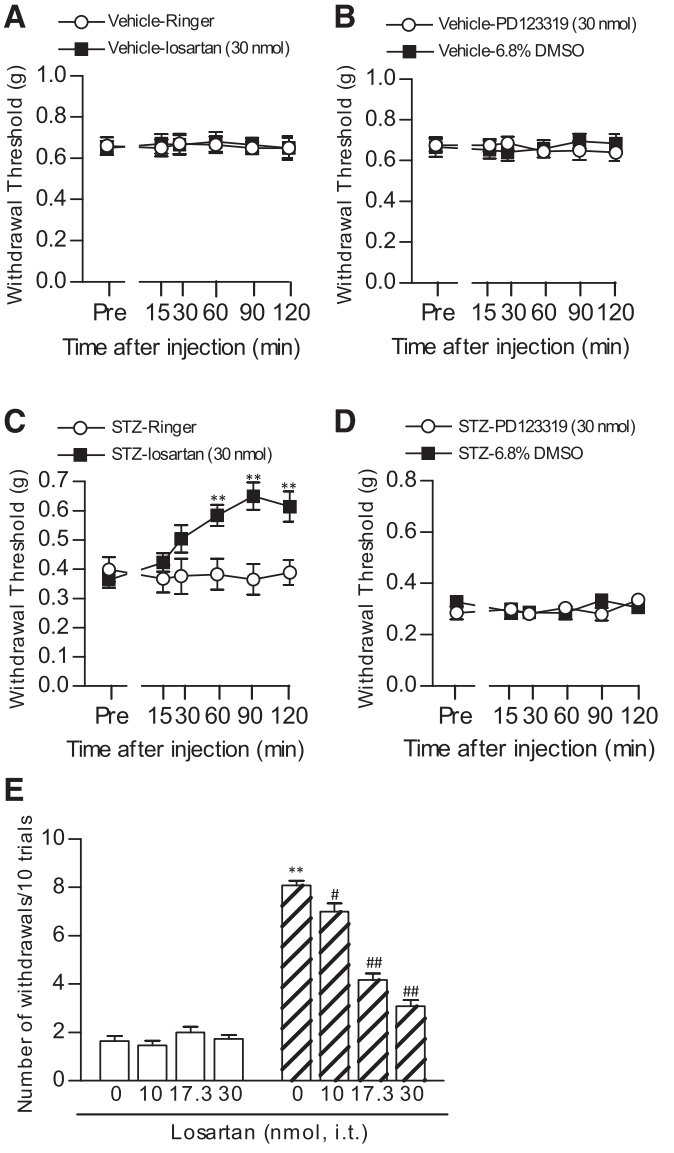

Fig. 2. Effects of Ang II receptor antagonists on tactile allodynia in STZ mice. Tactile allodynia was measured on day 14 after STZ (200 mg/kg) injection. Time courses of the effect of intrathecal administration of losartan (A, C) or PD123319 (B, D) on paw withdrawal responses to von Frey filaments in vehicle or STZ mice. (A) Two-way ANOVA: losartan treatment ($F_{1,18} = 0.04$, $P > 0.05$); time ($F_{5,90} = 0.08$, $P > 0.05$); losartan treatment × time ($F_{5,90} = 0.04$, $P > 0.05$). (B) Two-way ANOVA: PD123319 treatment ($F_{1,21} = 0.12$, $P > 0.05$); time ($F_{5,105} = 1.17$, $P > 0.05$); PD123319 treatment × time ($F_{5,105} = 2.18$, $P > 0.05$). (C) Two-way ANOVA: losartan treatment ($F_{1,31} = 7.69$, $P < 0.01$); time ($F_{5,155} = 6.39$, $P < 0.01$); losartan treatment × time ($F_{5,155} = 7.49$, $P < 0.01$). One-way ANOVA: $F_{7,88} = 109.56$, $P < 0.01$. (D) Two-way ANOVA: PD123319 treatment ($F_{1,21} = 0.12$, $P > 0.05$); time ($F_{5,105} = 1.17$, $P > 0.05$); PD123319 treatment × time ($F_{5,105} = 2.18$, $P > 0.05$). Values represent the mean ± S.E.M. for 10–20 mice. $^{**}P < 0.01$ compared with Ringer controls. (E) Dose-response effect of the intrathecal injection of losartan on the frequency of paw withdrawal responses to 0.4 g tactile stimuli in vehicle and STZ mice. Losartan or Ringer's solution was administered 90 minutes prior to measurements. Two-way ANOVA: dose ($F_{1,22} = 765.32$, $P < 0.01$); group ($F_{3,66} = 77.10$, $P < 0.01$); dose × group ($F_{3,66} = 43.51$, $P < 0.01$). One-way ANOVA: $F_{7,88} = 109.56$, $P < 0.01$. Values represent the mean ± S.E.M. for 12 mice. $^{**}P < 0.01$ compared with Ringer-injected vehicle mice and $\#P < 0.05$, $\#\#P < 0.01$ compared with Ringer-injected STZ mice.

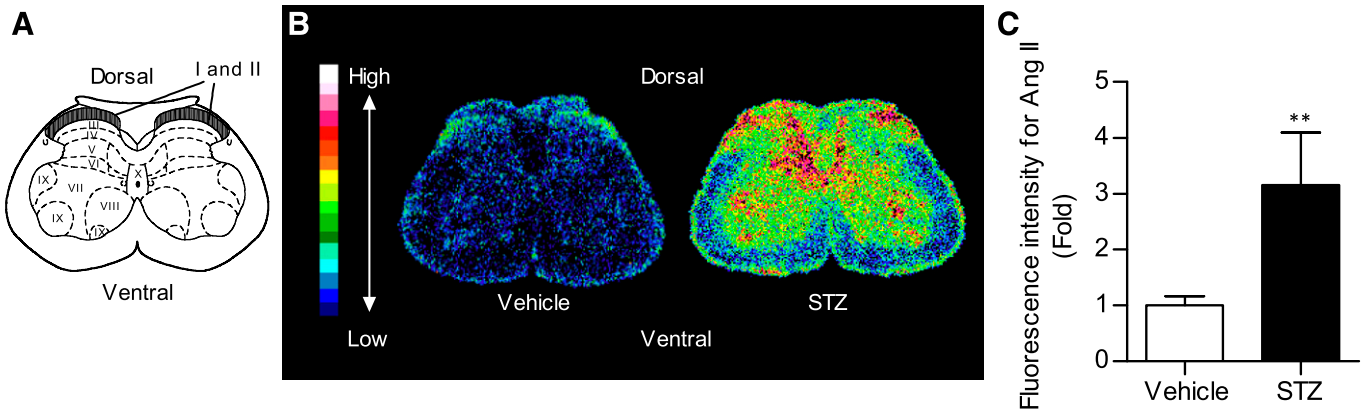

Fig. 3. Change in Ang II levels in the lumbar spinal cord of STZ mice. Immunofluorescence intensity for Ang II was measured on day 14 after STZ (200 mg/kg) injection. (A) Diagram representing segment L5 of the spinal cord. (B) Distribution of the immunohistochemical intensity for Ang II in the lumbar spinal cord of vehicle or STZ mice. (C) Quantification of the fluorescence intensity for Ang II relative to the superficial dorsal horn (laminae I and II) of vehicle mice. Values represent the mean ± S.E.M. for groups of 5–6 mice. $^{**}P < 0.01$ compared with vehicle.

rabbit antibodies against p38 MAPK, phospho-p38 MAPK, ACE, AGT, AT1 receptor, or β-actin (diluted 1:1000 with TBST containing 5% skim milk) at 4°C overnight. Blots were then washed several times and incubated at room temperature for 2 hours with horseradish peroxidase–conjugated anti-rabbit IgG antibody (1:5000 with TBST containing 5% skim milk). An ECL assay kit was used to develop the blots and immunoreactive (IR) proteins were visualized on Hyper-film ECL. The densities of the corresponding bands were analyzed using Image-J 1.43u (National Institutes of Health).

RT-PCR

Total RNA was isolated from the spinal cord, kidney, and liver of nontreated mice using TRI Reagent according to the manufacturer

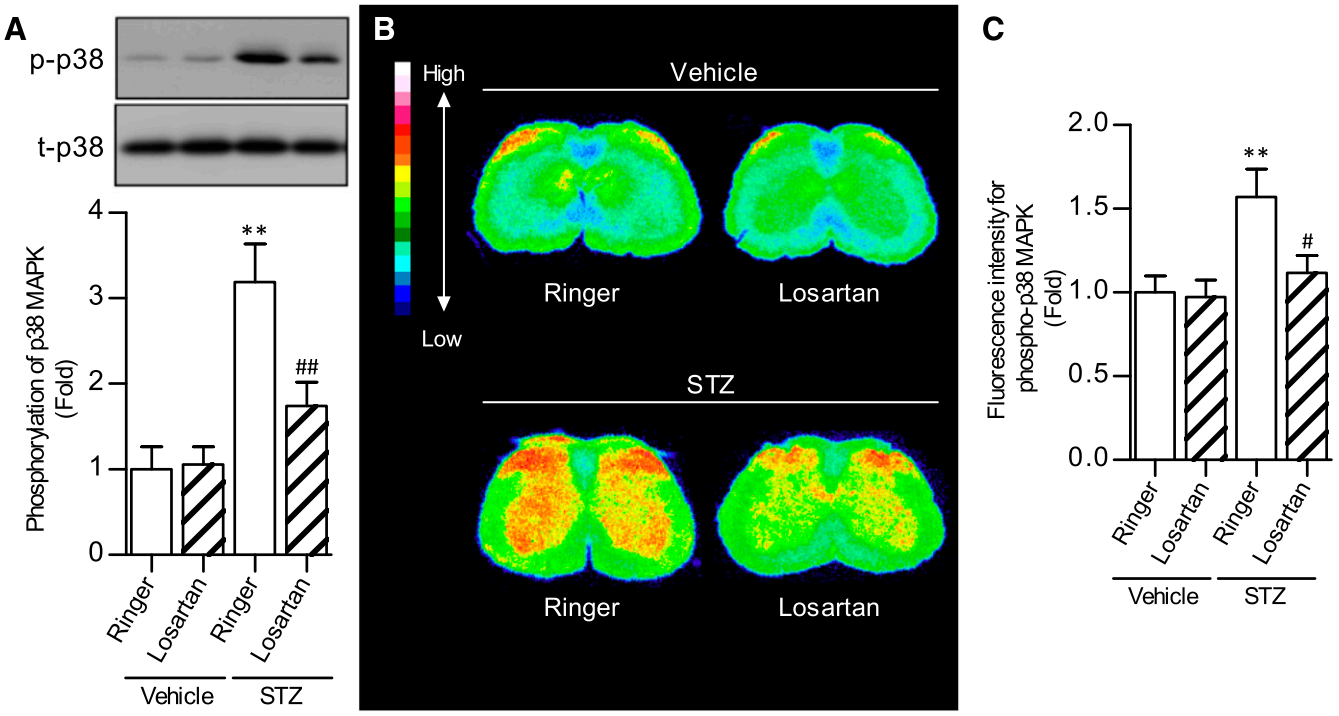

Fig. 4. Change in phospho-p38 MAPK levels in the lumbar spinal cord of STZ mice and the effect of losartan. Phospho-p38 MAPK was measured on day 14 after STZ (200 mg/kg) injection. (A) Phosphorylation of p38 MAPK by Western blotting. Dorsal lumbar spinal cord samples were taken 90 minutes after intrathecal injection of losartan (30 nmol) or Ringer's solution. (Top) Representative Western blot showing phospho- and total-p38 MAPK. (Bottom) Relative quantification of phospho-p38 MAPK to total-p38 MAPK set as 1.0 in the Ringer's solution–injected vehicle mice. Two-way ANOVA: group ($F_{1,17} = 24.91, P < 0.01$); losartan treatment ($F_{1,17} = 5.82, P < 0.05$); group × losartan treatment ($F_{1,17} = 6.87, P < 0.05$). One-way ANOVA: $F_{3,17} = 11.14$, $P < 0.01$. Values represent the mean ± S.E.M. for groups of 4–6 mice. $^{**}P < 0.01$ compared with Ringer's solution–injected vehicle mice, $^{\#\#}P < 0.01$ compared with Ringer's solution–treated STZ mice. (B) Distribution of the immunohistochemical intensity for phospho-p38 MAPK in the lumbar spinal cord. Losartan or Ringer's solution was intrathecal administered 90 minutes prior to fixative perfusion. (C) Quantification of the fluorescence intensity for phospho-p38 MAPK relative to the superficial dorsal horn (laminae I and II) of Ringer's solution–treated vehicle mice. Two-way ANOVA: group ($F_{1,30} = 5.35, P < 0.05$); losartan treatment ($F_{1,30} = 13.72, P < 0.01$); group × losartan treatment ($F_{1,30} = 10.69, P < 0.01$). One-way ANOVA: $F_{3,30} = 5.10$, $P < 0.01$. Each value represents the mean ± S.E.M. of 4–6 mice. $^{**}P < 0.01$ compared with Ringer's solution–treated vehicle mice; $^{\#}P < 0.05$ compared with Ringer's solution–treated STZ mice.

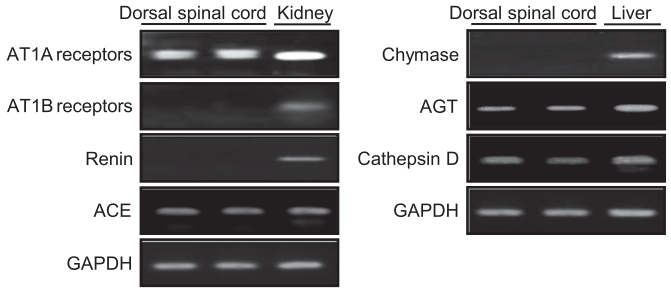

Fig. 5. Expression of RAS components mRNA in the mouse spinal cord. Total RNA was extracted from the lumbar dorsal spinal cord, kidney, and liver of untreated mice. RT-PCR was performed using a primer corresponding to mouse AT1A receptors, AT1B receptors, renin, ACE, chymase, AGT, or cathepsin D. GAPDH was used as a control for expression.

protocol. Total RNA was reverse transcribed using ReverTraAce and oligo (dT) primers. PCR was conducted using the following primer sequences: AT1A receptor sense primer 5′-TTG AAG AAG TAA TTA TGC AAA GCT G-3′ and antisense primer 5′-GAC ACG TGG GTC TCC ATT G-3′ [280 base pair (bp) product]; AT1B receptor sense primer 5′-CTG CTA TGC CCA TCA CCA TCT G-3′ and antisense primer 5′-GAT AAC CCT GCA TGC GAC CTG-3′ (148 bp product); AGT sense primer 5′-ACA GCA TCT CGG TGT CTG TG-3′ and antisense primer 5′-TGT CGA GAT CTG AGG TGC AG-3′ (153 bp product); ACE sense primer 5′-ACA TAC CCT AGC TGA GCC TTC-3′ and antisense primer 5′-GTC GGT GTT AGA CAC TGG GTA-3′ (108 bp product); renin sense primer 5′-GAT CTT ATC TCC CCC GTG GT-3′ and antisense primer 5′-CCT GAT CCG TAG TGG ATG GT-3′ (245 bp product); chymase sense primer 5′-GCC CAA GGC ATT GCA TCC TA-3′ and antisense primer 5′-TCG CAT GGC ACA CAA AAC CT-3′ (177 bp product); cathepsin D sense primer 5′-GTG CCT CTT ATC CAG GGT GA-3′ and antisense primer 5′-ATT CCC ATG AAG CCA CTC AG-3′ (167 bp product); and glyceraldehyde-3-phosphate dehydrogenase (GAPDH) sense primer 5′-ACC ACA GTC CAT GCC ATC AC-3′ and antisense primer 5′-TCC ACC ACC CTG TTG CTG TA-3′ (166 bp product). To assess the PCR products qualitatively, an aliquot from each reaction was separated by electrophoresis on agarose gel and stained with ethidium bromide. A digital image of each gel was captured using FAS-III (Toyobo). For quantification of mRNA expression, real-time PCR was carried out in a 20-μl solution containing Go Taq quantitative PCR Master mix (10 μl), RT template (2 μl), water (7 μl), and primers (1 μl) using the StepOnePlus Real-Time PCR System (Applied Biosystems, Foster City, CA). The amount of each PCR product was normalized to GAPDH.

Statistical Methods

Data are expressed as the mean ± SEM. Significant differences were analyzed by one-way or two-way analysis of variance (ANOVA), followed by Fisher's protected least significant difference test for multiple comparisons. The Student's t test was used for comparisons between two groups. Statistical significance was considered at $P < 0.05$ in all comparisons.

Results

Time Course of Blood Glucose Levels, Body Weight, and Tactile Allodynia Up to 28 Days After STZ Injection. Blood glucose levels, body weights, and tactile allodynia were measured at 1, 3, 5, 7, 14, 21, and 28 days after mice received injections of STZ (2–200 mg/kg) or vehicle (citrate buffer). Blood glucose levels were significantly increased in STZ (200 mg/kg)-treated mice (from 190 to 280 mg/dl) compared with those of vehicle-treated mice 1 day after injection, and rose above the detection limit of the meter (>500 mg/dL), where they remained from day 7 onward (Fig. 1A). Such increases in glucose levels after STZ injection confirmed the induction of a diabetic state. On the other hand, 2 and 20 mg/kg doses of STZ did not affect blood glucose levels (Fig. 1A). The rate of increase in body weight in STZ (200 mg/kg)-induced diabetic mice (STZ mice) was slower than in vehicle- or STZ-treated mice at 2 and 20 mg/kg throughout the experimental period (Fig. 1B).

STZ mice are widely used as models of diabetic neuropathic pain. However, it has been shown that STZ can directly stimulate DRG neurons and induce thermal hyperalgesia without affecting blood glucose levels (Pabbidi et al., 2008). Concurrent with the increase in blood glucose levels, a significant decrease in the withdrawal threshold was observed 1 day after treatment with 200 mg/kg STZ (Fig. 1C), and this remained the same throughout the entire experimental period. In addition, blood glucose levels were not affected by STZ doses of 2 and 20 mg/kg, whereas the withdrawal threshold was significantly decreased on day 1 only and on days 1–3 after injection, respectively (Fig. 1C). Therefore, to exclude the possibility that STZ has a direct action on neurons, we used mice on day 14 after injection at 200 mg/kg, which was a point in time that showed a marked decrease in pain threshold.

Effects of Ang II Receptor Antagonists on STZ-Induced Tactile Allodynia. To investigate whether spinal Ang II receptors are involved in STZ-induced tactile allodynia, the effects of intrathecal administration of losartan or PD13319, which are AT1 and AT2 receptor antagonists, respectively, were examined on day 14 after STZ injection.

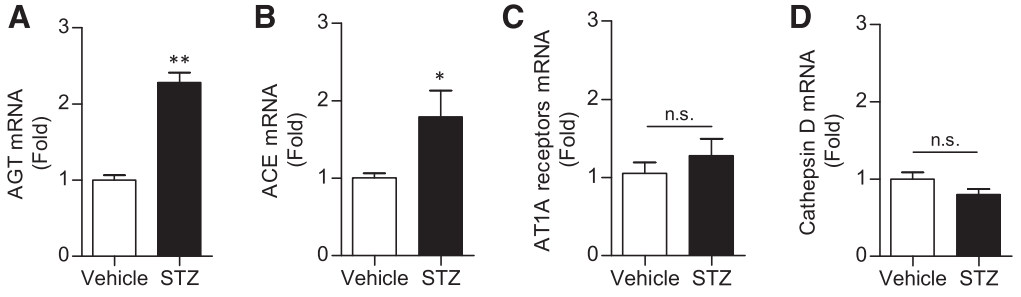

Fig. 6. Changes in the expression of spinal mRNAs for Ang II–generating system genes in the STZ mice. Determination of the relative levels of AGT, ACE, AT1A receptors, and cathepsin D mRNA by real-time RT-PCR in the mouse lumbar dorsal spinal cord. Dorsal spinal cord samples were extracted on day 14 after STZ (200 mg/kg) injection. Total RNA was assessed for AGT (A), ACE (B), AT1A receptors (C), or cathepsin D (D) mRNA expression by real-time RT-PCR. Values represent the mean ± S.E.M. for groups of 5–6 mice. *$P < 0.05$, **$P < 0.01$ compared with vehicle controls.

Tactile allodynia was measured before and after (15, 30, 60, 90, and 120 minutes) intrathecal injection. In vehicle-treated mice, losartan did not affect the withdrawal threshold at any time throughout the experimental period (Fig. 2A). Similarly, PD123319 showed no significant effects (Fig. 2B). On the other hand, tactile allodynia was significantly inhibited 60–120 minutes after intrathecal administration of losartan (30 nmol) in STZ mice compared with Ringer's solution–treated controls (Fig. 2C). In contrast, PD123319 (30 nmol) did not have any significant effects on STZ-induced tactile allodynia (Fig. 2D), although it has been shown to significantly reduce the pressor effect induced by intrathecal administration of Ang II at a lower dose of 13.6 nmol (Park and Henry, 1997).

We additionally examined the dose dependency of losartan (10–30 nmol) on STZ-induced tactile allodynia 90 minutes after administration. As shown in Fig. 2E, losartan (10–30 nmol) inhibited STZ-induced tactile allodynia in a dose-dependent manner. Taken together, these results suggest that spinal AT1, but not AT2, receptors are involved in STZ-induced tactile allodynia.

Levels of Ang II in the Lumbar Spinal Cord of STZ Mice. To examine whether spinal Ang II levels are increased in STZ mice, the distribution of Ang II immunofluorescence intensity was determined by microphotometry and categorized according to 18 levels (shown by colors in Fig. 3B, where the lowest concentration is black, and the highest concentration is white). Relatively high fluorescence intensities for Ang II were seen in the lumbar superficial dorsal horn (laminae I and II) in vehicle mice (Fig. 3B). Importantly, these intensities increased by approximately threefold in STZ mice, indicating a potential increase in local RAS activity (Fig. 3C).

Phosphorylation of p38 MAPK in the Lumbar Spinal Cord of STZ Mice. To investigate whether spinal p38 MAPK is activated in STZ mice, we examined the phosphorylation of p38 MAPK in the lumbar dorsal cord by Western blotting. There was a marked increase in the phosphorylation of p38 MAPK in STZ mice (Fig. 4A). However, intrathecal administration of losartan (30 nmol) had a significant preventive effect on this increase (Fig. 4A). High fluorescence intensity for phospho-p38 MAPK was seen in the lumbar

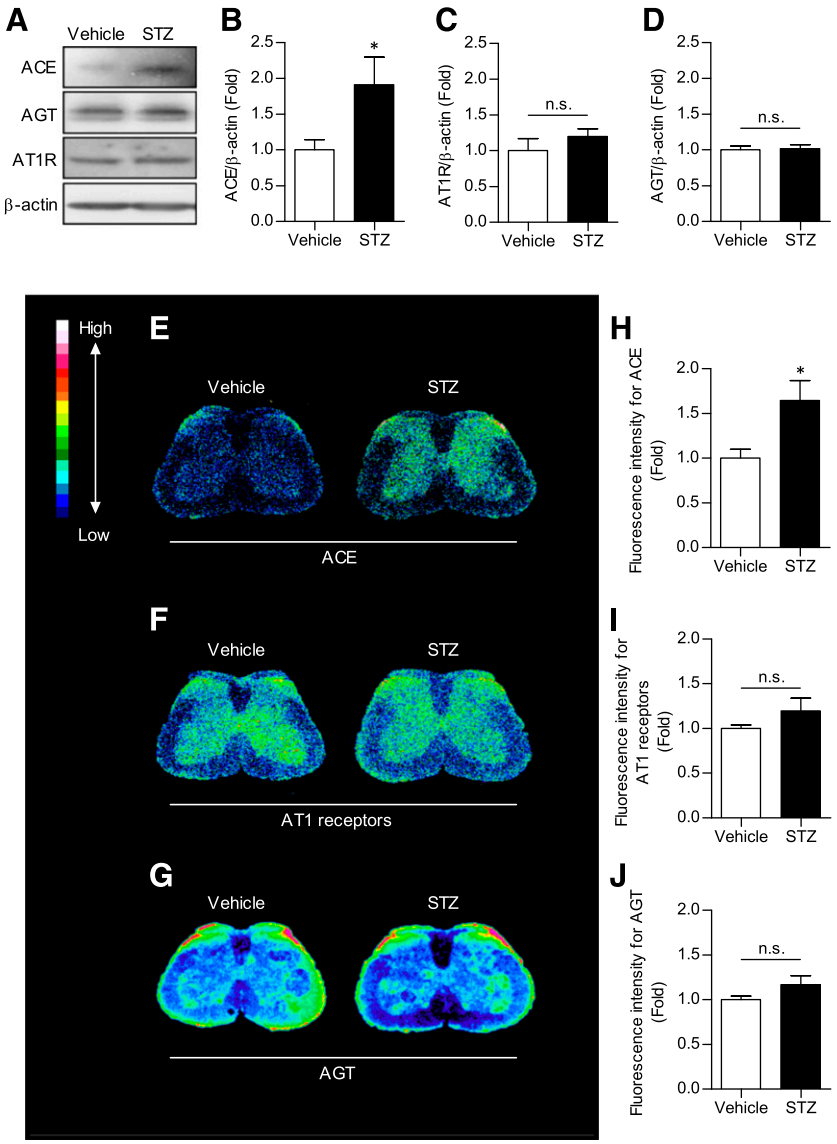

Fig. 7. Changes in ACE, AT1 receptors and AGT levels in the lumbar spinal cord of STZ mice. (A) Representative Western blots showing ACE, AT1 receptors, AGT, and β-actin. Dorsal lumbar spinal cord samples were taken 14 days after STZ (200 mg/kg) injection. (B–D) Relative quantification of ACE (B), AT1 receptors (C), and AGT (D) to β-actin set as 1.0 in the vehicle mice. Each value represents the mean ± S.E.M. of 5–6 mice. $^*P < 0.05$ compared with vehicle controls. Immunofluorescence intensities were measured on day 14 after STZ (200 mg/kg) injection. Distribution of the immunohistochemical intensity for ACE (E), AT1 receptors (F), and AGT (G) in the lumbar spinal cord of STZ mice. Quantification of the fluorescence intensity for ACE (H), AT1 receptors (I), and AGT (J) relative to the superficial dorsal horn (laminae I and II) of vehicle mice. Values represent the mean ± S.E.M. for groups of 4–8 mice. $^*P < 0.05$, compared with vehicle. n.s., nonsignificant.

superficial dorsal horn of Ringer-injected STZ mice (Fig. 4B). Furthermore, the intensity was increased approximately 1.5-fold in Ringer-injected STZ mice compared with Ringer-injected vehicle mice, and was significantly attenuated by losartan (Fig. 4C).

Expression of mRNA of RAS Components in the Mouse Spinal Cord. To investigate whether RAS components are expressed in the mouse lumbar dorsal spinal cord, the presence of transcripts were determined by RT-PCR. The mRNAs for AT1A receptors, ACE, AGT, and cathepsin D were expressed in the lumbar dorsal spinal cord (Fig. 5), whereas those for AT1B receptor, renin, and chymase were not detected. The kidney and liver were used as positive controls for PCR detection.

Next, we determined the levels of AT1A receptors, ACE, AGT, and cathepsin D mRNA expression in the lumbar dorsal spinal cord of STZ mice using real-time quantitative RT-PCR. Both AGT and ACE transcripts were significantly increased in STZ mice compared with vehicle mice (Fig. 6, A and B). In contrast, the mRNA levels for AT1A receptor and cathepsin D did not differ significantly between STZ and vehicle mice (Fig. 6, C and D).

Levels of ACE, AT1 Receptors, and AGT in the Lumbar Spinal Cord of STZ Mice. We determined the levels of ACE, AT1 receptors, and AGT in the lumbar dorsal spinal cord of STZ mice by Western blotting. Spinal ACE increased significantly in STZ mice compared with vehicle mice (Fig. 7, A and B). On the other hand, the levels of AGT and AT1 receptors did not significantly differ between STZ and vehicle mice (Fig. 7, A, C, and D). Moreover, to quantify the levels of these RAS components in the superficial dorsal horn, we performed immunohistochemical labeling and measured the intensity of fluorescence in laminae I and II using MapAnalyzer. The distribution of ACE, AT1 receptors, and AGT in the mouse lumbar spinal cord and their immunofluorescence intensities are shown in Fig. 7, E–G. Relatively high fluorescence intensities for ACE, AT1 receptors, and AGT were seen in vehicle mice. In addition, the fluorescence intensity for ACE in the superficial dorsal horn had increased by approximately 1.7-fold in the STZ mice compared with vehicle mice (Fig. 7H). However, the intensities of AT1 receptors (Fig. 7I) and AGT (Fig. 7J) in diabetic mice did not differ from those of vehicle mice.

Dual Immunolabeling of ACE and Cell-Specific Markers in the Mouse Lumbar Superficial Dorsal Horn. Dual-immunofluorescence staining for ACE was performed in conjunction with that for cell-specific markers—NeuN for neurons, GFAP for astrocytes, and Iba-1 for microglia—to determine the cell types that are involved in the production of Ang II. ACE was localized in NeuN-IR cells (Fig. 8, A–C), whereas it was absent in GFAP-IR and Iba-1-IR cells (Fig. 8, D–I). These results indicated that ACE is expressed in neurons, but not in astrocytes or microglial cells in the mouse superficial dorsal horn.

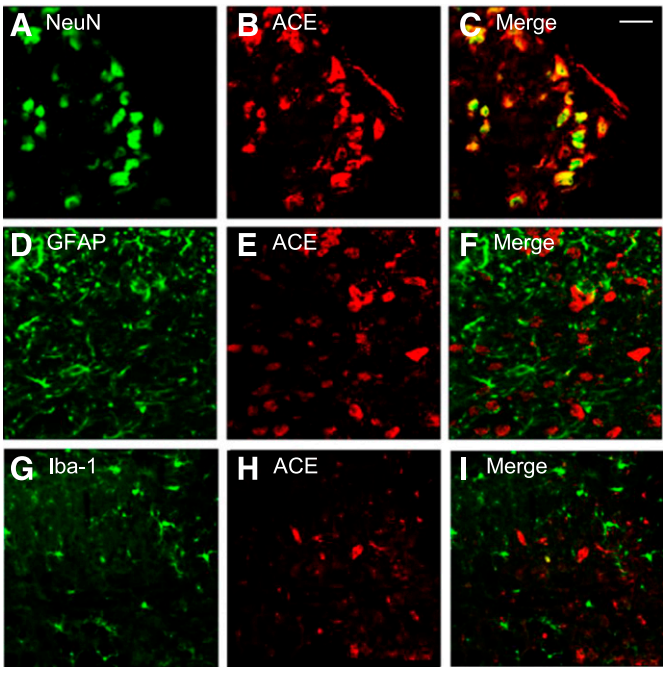

Fig. 8. Double-immunofluorescence staining of ACE and either NeuN, GFAP, or Iba-1 in the mouse lumbar superficial dorsal horn (L5). Photomicrographs of fluorescent NeuN-IR cells (A) and ACE-IR cells (B), and the merging of (A) and (B) (C). Photomicrographs of fluorescent GFAP-IR cells (D) and ACE-IR cells (E), and the merging of (D) and (E) (F). Photomicrographs of fluorescent Iba-1-IR cells (G) and ACE-IR cells (H), and the merging of (G) and (H) (I). Scale bar, 20 μm.

Discussion

We have previously reported that Ang II may act as a neurotransmitter and/or neuromodulator in the spinal transmission of nociceptive information (Nemoto et al., 2013, 2015a, 2015b). The involvement of the RAS in diabetic nephropathy and retinopathy has been demonstrated alongside the beneficial effects on these complications by treatment with ACE inhibitors or AT1 receptor antagonists (Carey and Siragy, 2003; Nagai et al., 2007). Coppey et al. (2006) have shown that treatment with either enalapril, an ACE inhibitor, or L-158809, an AT1 receptor antagonist, prevents or reverses diabetic neuropathy in STZ-induced diabetic rats (STZ rats). Although the evidence indicates that RAS activity is increased in diabetes (Van Dyk et al., 1994; van Dijk et al., 2001), the role of spinal RAS on diabetic neuropathic pain has not been reported to date. Thus, we hypothesized that it was important to examine whether spinal RAS is necessary and sufficient for diabetic neuropathic pain in the STZ mouse model.

STZ is the most common agent used to induce experimental type 1 diabetic syndrome in animals. STZ is taken up by the β-cells of the islets of Langerhans in the pancreas via glucose transporter-2, which leads to their destruction and elevated plasma glucose levels (Schnedl et al., 1994; Szkudelski, 2001). In this study, a single intravenous injection of STZ (200 mg/kg) caused a rapid onset of hyperglycemia within 24 hours. The blood glucose levels remained markedly elevated even on day 28 after injection. A sudden increase in blood glucose level can cause structural and functional changes in the nerves, and possibly neuropathic pain (Boulton, 1992; Tesfaye et al., 1996). Moreover, the development of STZ-induced diabetic neuropathic pain is prevented by pretreatment with insulin (Aley and Levine, 2001; Messinger et al., 2009). These previous reports suggest that STZ-induced diabetic neuropathic pain may be frequently associated with hyperglycemia. In our study, lower doses of STZ (2 and 20 mg/kg) had no effect on blood glucose levels, whereas the withdrawal threshold was only briefly decreased to a significant level (on days 1–3) after

injection. To exclude the possibility that STZ has a direct action on neurons, as reported previously (Pabbidi et al., 2008), we used STZ (200 mg/kg)-injected mice with altered blood glucose levels from a later time point (day 14) as our model for diabetes-induced neuropathic pain.

Oral administration of an Ang II receptor antagonist or ACE inhibitor increases motor nerve conduction velocity, and is decreased in STZ rats without affecting blood glucose levels (Coppey et al., 2006). This suggests that blocking the activation of the RAS provides an effective approach toward the prevention/reversal of diabetes-induced neuronal dysfunction. In addition, it has been shown that oral administration of telmisartan, an AT1 receptor antagonist, has the potential to attenuate neuropathic pain in a chronic constriction injury model (Jaggi and Singh, 2011). In the present study, the fluorescence intensity for Ang II in the superficial dorsal horn of the spinal cord increased significantly on day 14 after STZ injection compared with vehicle-treated controls. Intrathecal administration of losartan reversed the tactile allodynia observed significantly and led to a dose-dependent decrease in the number of withdrawal responses on day 14 after injection of STZ. In contrast, the AT2 receptor antagonist PD123319 had no effect on STZ-induced tactile allodynia. Moreover, STZ-induced increases in phospho-p38 MAPK in the superficial dorsal horn of STZ mice were significantly inhibited by intrathecal administration of losartan. A Ser/Thr kinase, p38 MAPK, which converts extracellular stimuli into a wide range of cellular responses, plays an important role in spinal nociceptive transmission. For example, spinal p38 MAPK is phosphorylated in neuropathic pain models, such as chronic constriction injury or spinal nerve ligation, whereas intrathecal administration of p38 MAPK inhibitors attenuates tactile allodynia in these models (Tsuda et al., 2004; Xu et al., 2007). The phosphorylation of p38 MAPK is also seen in STZ rats, and p38 MAPK inhibitors reverse or prevent neuropathic pain (Daulhac et al., 2006). In our previous study, the phosphorylation of p38 MAPK induced by intrathecal administration of Ang II in mice was seen in spinal astrocytes and neurons, both of which can express AT1 receptors (Nemoto et al., 2015a). These findings suggest that losartan inhibits the phosphorylation of astrocytic and neuronal p38 MAPK in the superficial dorsal horns of diabetic mice. We have reported that intrathecal administration of Ang II induces nociceptive behavior alongside phosphorylation of spinal p38 MAPK (Nemoto et al., 2013, 2014, 2015a). Both nociceptive behavior and an increase in p38 MAPK phosphorylation have been shown to be mediated through AT1, but not AT2, receptors (Nemoto et al., 2013). Moreover, the injection of 2% formalin into the mouse hind paw increases the fluorescence intensity for Ang II on the ipsilateral side of the lumbar superficial dorsal horn. Furthermore, losartan dose-dependently protects against the nociceptive effect by inhibiting p38 MAPK phosphorylation (Nemoto et al., 2015b). Collectively, these findings suggest that STZ-induced diabetic neuropathic pain involves the activation of p38 MAPK signaling mediated by AT1, but not AT2, receptors in spinal astrocytes and neurons.

ACE and AGT are expressed in the pineal gland, diencephalon, brain stem, cortex, and cerebellum (Baltatu et al., 1998), whereas Ang II is locally synthesized in the brain (Ganten et al., 1983). However, Ang II has not yet been reported to be locally synthesized in the spinal cord. Therefore, we examined whether the local Ang II–generating system is present in the mouse lumbar dorsal spinal cord, and found mRNAs for AGT, ACE, and cathepsin D, an enzyme homologous to renin (Morris and Reid, 1978), but not that for renin. Moreover, renin mRNA was not detected in the lumbar dorsal spinal cord of STZ mice (data not shown). Although chymase can form Ang II by cleaving Ang I (Kirimura et al., 2005), its mRNA was also absent from the lumbar dorsal spinal cord. Similar to the spinal cord, the mRNA for cathepsin D, but not renin, is reported to be expressed in the DRG (Patil et al., 2010). Therefore, we can speculate that cathepsin D cleaves AGT to Ang I, which is in turn converted to Ang II by ACE in the spinal cord.

It has been reported that renin gene expression and AT1 receptor protein synthesis are increased, whereas the expression levels of AGT and ACE mRNAs remain unchanged, in the proximal tubules of STZ rats (Zimpelmann et al., 2000). On the other hand, an increase in AGT mRNA leading to the upregulation of Ang II has been observed in the retinae of STZ mice (Ebrahimian et al., 2005). These reports indicate that several local Ang II–generating system components are increased in diabetes, depending on the organ or tissue under investigation. In this study, the expression of both AGT and ACE genes was increased in the lumbar dorsal spinal cord of STZ mice, whereas there was no change in cathepsin D expression. However, at the protein level, only ACE was increased in a significant manner, whereas AGT was not changed. Moreover, we observed that spinal ACE is present in neurons but is absent from glial cells in the superficial dorsal spinal cord. Therefore, the present results suggest that only the expression of ACE was increased, and among the local Ang II-generating system components in the spinal cord of the STZ mice, it was responsible for the increase in Ang II levels.

Regarding the expression of AT1 receptors, only transcripts for AT1A but not AT1B subtypes were expressed in the mouse lumbar dorsal spinal cord. Most species express a single type of AT1 receptor, but rodents express two isoforms, AT1A and AT1B (Timmermans et al., 1993). These isoforms share approximately 96% amino acid sequence homology and have similar ligand-binding affinities (Iwai and Inagami, 1992; Yoshida et al., 1992). In the lumbar dorsal spinal cord of STZ mice, neither the expression of AT1 receptor gene nor protein levels changed, though the immunofluorescence intensity for Ang II increased. It has been demonstrated that Ang II decreases AT1 receptor expression in proximal tubule cells in rats (Zeng et al., 2003). In the STZ mouse model, the local expression levels of AT1A receptor mRNA and AT1 receptors may not be influenced by the increase in Ang II in the spinal cord.

In conclusion, our data show that a local Ang II–generating system is present in the spinal cord. Among local components, the expression of ACE was increased in STZ-induced diabetic mice, which led to an increase in Ang II levels. Moreover, this increase in Ang II caused tactile allodynia accompanied by the phosphorylation of p38 MAPK via AT1 receptors in the lumbar superficial dorsal horn.

Acknowledgments

The authors thank Daichi Hasegawa, Aya Ohori, Yoshiko Shimawaki, and Shiori Hino at Tohoku Medical and Pharmaceutical University for their technical assistance.

Authorship Contributions

Participated in research design: Tadano and Tan-No.

Conducted experiments: Ogata, Nemoto, Nakagawasai, and Yamagata.

Performed data analysis: Ogata, Nemoto, and Nakagawasai.

Wrote or contributed to the writing of the manuscript: Ogata, Nemoto, and Tan-No.

References

Aley KO and Levine JD (2001) Rapid onset pain induced by intravenous streptozotocin in the rat. *J Pain* **2**:146–150.

Bader M (2010) Tissue renin-angiotensin-aldosterone systems: targets for pharmacological therapy. *Annu Rev Pharmacol Toxicol* **50**:439–465.

Baltatu O, Lippoldt A, Hansson A, Ganten D, and Bader M (1998) Local renin-angiotensin system in the pineal gland. *Brain Res Mol Brain Res* **54**:237–242.

Boulton A (1992) What causes neuropathic pain? *J Diabetes Complications* **6**:58–63.

Boulton AJ, Vinik AI, Arezzo JC, Bril V, Feldman EL, Freeman R, Malik RA, Maser RE, Sosenko JM, and Ziegler D; American Diabetes Association (2005) Diabetic neuropathies: a statement by the American Diabetes Association. *Diabetes Care* **28**:956–962.

Burkhalter J, Felix D, and Imboden H (2001) A new angiotensinergic system in the CNS of the rat. *Regul Pept* **99**:93–101.

Campbell DJ (2014) Clinical relevance of local renin angiotensin systems. *Front Endocrinol (Lausanne)* **5**:113.

Carey RM and Siragy HM (2003) The intrarenal renin-angiotensin system and diabetic nephropathy. *Trends Endocrinol Metab* **14**:274–281.

Coppey LJ, Davidson EP, Rinehart TW, Gellett JS, Oltman CL, Lund DD, and Yorek MA (2006) ACE inhibitor or angiotensin II receptor antagonist attenuates diabetic neuropathy in streptozotocin-induced diabetic rats. *Diabetes* **55**:341–348.

Daousi C, MacFarlane IA, Woodward A, Nurmikko TJ, Bundred PE, and Benbow SJ (2004) Chronic painful peripheral neuropathy in an urban community: a controlled comparison of people with and without diabetes. *Diabet Med* **21**:976–982.

Daulhac L, Mallet C, Courteix C, Etienne M, Duroux E, Privat AM, Eschalier A, and Fialip J (2006) Diabetes-induced mechanical hyperalgesia involves spinal mitogen-activated protein kinase activation in neurons and microglia via N-methyl-D-aspartate-dependent mechanisms. *Mol Pharmacol* **70**:1246–1254.

Dyck PJ, Kratz KM, Karnes JL, Litchy WJ, Klein R, Pach JM, Wilson DM, O'Brien PC, Melton LJ, 3rd, and Service FJ (1993) The prevalence by staged severity of various types of diabetic neuropathy, retinopathy, and nephropathy in a population-based cohort: the Rochester Diabetic Neuropathy Study. *Neurology* **43**:817–824.

Ebrahimian TG, Tamarat R, Clergue M, Duriez M, Levy BI, and Silvestre JS (2005) Dual effect of angiotensin-converting enzyme inhibition on angiogenesis in type 1 diabetic mice. *Arterioscler Thromb Vasc Biol* **25**:65–70.

Ganten D, Hermann K, Bayer C, Unger T, and Lang RE (1983) Angiotensin synthesis in the brain and increased turnover in hypertensive rats. *Science* **221**:869–871.

Gordois A, Scuffham P, Shearer A, Oglesby A, and Tobian JA (2003) The health care costs of diabetic peripheral neuropathy in the US. *Diabetes Care* **26**:1790–1795.

Hollenberg NK, Price DA, Fisher ND, Lansang MC, Perkins B, Gordon MS, Williams GH, and Laffel LM (2003) Glomerular hemodynamics and the renin-angiotensin system in patients with type 1 diabetes mellitus. *Kidney Int* **63**:172–178.

Iwai N and Inagami T (1992) Identification of two subtypes in the rat type I angiotensin II receptor. *FEBS Lett* **298**:257–260.

Jaggi AS and Singh N (2011) Exploring the potential of telmisartan in chronic constriction injury-induced neuropathic pain in rats. *Eur J Pharmacol* **667**:215–221.

Kamei J, Ohhashi Y, Aoki T, and Kasuya Y (1991) Streptozotocin-induced diabetes in mice reduces the nociceptive threshold, as recognized after application of noxious mechanical stimuli but not of thermal stimuli. *Pharmacol Biochem Behav* **39**:541–544.

Kirimura K, Takai S, Jin D, Muramatsu M, Kishi K, Yoshikawa K, Nakabayashi M, Mino Y, and Miyazaki M (2005) Role of chymase-dependent angiotensin II formation in regulating blood pressure in spontaneously hypertensive rats. *Hypertens Res* **28**:457–464.

Kobori H, Nangaku M, Navar LG, and Nishiyama A (2007) The intrarenal renin-angiotensin system: from physiology to the pathobiology of hypertension and kidney disease. *Pharmacol Rev* **59**:251–287.

Leehey DJ, Singh AK, Alavi N, and Singh R (2000) Role of angiotensin II in diabetic nephropathy. *Kidney Int Suppl* **77**:S93–S98.

Messinger RB, Naik AK, Jagodic MM, Nelson MT, Lee WY, Choe WJ, Orestes P, Latham JR, Todorovic SM, and Jevtovic-Todorovic V (2009) In vivo silencing of the Ca(V)3.2 T-type calcium channels in sensory neurons alleviates hyperalgesia in rats with streptozocin-induced diabetic neuropathy. *Pain* **145**:184–195.

Morris BJ and Reid IA (1978) A "renin-like" enzymatic action of cathepsin D and the similarity in subcellular distributions of "renin-like" activity and cathepsin D in the midbrain of dogs. *Endocrinology* **103**:1289–1296.

Nagai N, Izumi-Nagai K, Oike Y, Koto T, Satofuka S, Ozawa Y, Yamashiro K, Inoue M, Tsubota K, and Umezawa K et al. (2007) Suppression of diabetes-induced retinal inflammation by blocking the angiotensin II type 1 receptor or its downstream nuclear factor-kappaB pathway. *Invest Ophthalmol Vis Sci* **48**:4342–4350.

Nakagawasai O, Hozumi S, Tan-No K, Niijima F, Arai Y, Yasuhara H, and Tadano T (2003) Immunohistochemical fluorescence intensity reduction of brain somatostatin in the impairment of learning and memory-related behaviour induced by olfactory bulbectomy. *Behav Brain Res* **142**:63–67.

Nemoto W, Nakagawasai O, Yaoita F, Kanno S, Yomogida S, Ishikawa M, Tadano T, and Tan-No K (2013) Angiotensin II produces nociceptive behavior through spinal AT1 receptor-mediated p38 mitogen-activated protein kinase activation in mice. *Mol Pain* **9**:38.

Nemoto W, Ogata Y, Nakagawasai O, Yaoita F, Tadano T, and Tan-No K (2014) Angiotensin (1-7) prevents angiotensin II-induced nociceptive behaviour via inhibition of p38 MAPK phosphorylation mediated through spinal Mas receptors in mice. *Eur J Pain* **18**:1471–1479.

Nemoto W, Ogata Y, Nakagawasai O, Yaoita F, Tadano T, and Tan-No K (2015a) Involvement of p38 MAPK activation mediated through AT1 receptors on spinal astrocytes and neurons in angiotensin II- and III-induced nociceptive behavior in mice. *Neuropharmacology* **99**:221–231.

Nemoto W, Ogata Y, Nakagawasai O, Yaoita F, Tanado T, and Tan-No K (2015b) The intrathecal administration of losartan, an AT1 receptor antagonist, produces an antinociceptive effect through the inhibiton of p38 MAPK phosphorylation in the mouse formalin test. *Neurosci Lett* **585**:17–22.

Pabbidi RM, Cao DS, Parihar A, Pauza ME, and Premkumar LS (2008) Direct role of streptozotocin in inducing thermal hyperalgesia by enhanced expression of transient receptor potential vanilloid 1 in sensory neurons. *Mol Pharmacol* **73**: 995–1004.

Park PD and Henry JL (1997) Receptor subtypes mediating spinal cardiovascular effects of angiotensin II in rat using losartan and PD 123319. *Eur J Pharmacol* **326**:139–145.

Patil J, Schwab A, Nussberger J, Schaffner T, Saavedra JM, and Imboden H (2010) Intraneuronal angiotensinergic system in rat and human dorsal root ganglia. *Regul Pept* **162**:90–98.

Paul M, Poyan Mehr A, and Kreutz R (2006) Physiology of local renin-angiotensin systems. *Physiol Rev* **86**:747–803.

Pelegrini-da-Silva A, Martins AR, and Prado WA (2005) A new role for the renin-angiotensin system in the rat periaqueductal gray matter: angiotensin receptor-mediated modulation of nociception. *Neuroscience* **132**:453–463.

Schnedl WJ, Ferber S, Johnson JH, and Newgard CB (1994) STZ transport and cytotoxicity. Specific enhancement in GLUT2-expressing cells. *Diabetes* **43**: 1326–1333.

Szkudelski T (2001) The mechanism of alloxan and streptozotocin action in B cells of the rat pancreas. *Physiol Res* **50**:537–546.

Tesfaye S, Malik R, Harris N, Jakubowski JJ, Mody C, Rennie IG, and Ward JD (1996) Arterio-venous shunting and proliferating new vessels in acute painful neuropathy of rapid glycaemic control (insulin neuritis). *Diabetologia* **39**:329–335.

Timmermans PB, Wong PC, Chiu AT, Herblin WF, Benfield P, Carini DJ, Lee RJ, Wexler RR, Saye JA, and Smith RD (1993) Angiotensin II receptors and angiotensin II receptor antagonists. *Pharmacol Rev* **45**:205–251.

Tsuda M, Mizokoshi A, Shigemoto-Mogami Y, Koizumi S, and Inoue K (2004) Activation of p38 mitogen-activated protein kinase in spinal hyperactive microglia contributes to pain hypersensitivity following peripheral nerve injury. *Glia* **45**: 89–95.

van Dijk DJ, Boner G, Giler S, and Erman A (2001) Increased serum angiotensin-converting enzyme activity and plasma angiotensin II levels during pregnancy and postpartum in the diabetic rat. *J Renin Angiotensin Aldosterone Syst* **2**:193–198.

Van Dyk DJ, Erman A, Erman T, Chen-Gal B, Sulkes J, and Boner G (1994) Increased serum angiotensin converting enzyme activity in type I insulin-dependent diabetes mellitus: its relation to metabolic control and diabetic complications. *Eur J Clin Invest* **24**:463–467.

Veves A, Backonja M, and Malik RA (2008) Painful diabetic neuropathy: epidemiology, natural history, early diagnosis, and treatment options. *Pain Med* **9**: 660–674.

Vidotti DB, Casarini DE, Cristovam PC, Leite CA, Schor N, and Boim MA (2004) High glucose concentration stimulates intracellular renin activity and angiotensin II generation in rat mesangial cells. *Am J Physiol Renal Physiol* **286**:F1039–F1045.

Wu W, Zhang Y, Ballew JR, Fink G, and Wang DH (2000) Development of hypertension induced by subpressor infusion of angiotensin II: role of sensory nerves. *Hypertension* **36**:549–552.

Xu L, Huang Y, Yu X, Yue J, Yang N, and Zuo P (2007) The influence of p38 mitogen-activated protein kinase inhibitor on synthesis of inflammatory cytokine tumor necrosis factor alpha in spinal cord of rats with chronic constriction injury. *Anesth Analg* **105**:1838–1844.

Yoshida H, Kakuchi J, Guo DF, Furuta H, Iwai N, van der Meer-de Jong R, Inagami T, and Ichikawa I (1992) Analysis of the evolution of angiotensin II type 1 receptor gene in mammals (mouse, rat, bovine and human). *Biochem Biophys Res Commun* **186**:1042–1049.

Zeng C, Asico LD, Wang X, Hopfer U, Eisner GM, Felder RA, and Jose PA (2003) Angiotensin II regulation of AT1 and D3 dopamine receptors in renal proximal tubule cells of SHR. *Hypertension* **41**:724–729.

Zimpelmann J, Kumar D, Levine DZ, Wehbi G, Imig JD, Navar LG, and Burns KD (2000) Early diabetes mellitus stimulates proximal tubule renin mRNA expression in the rat. *Kidney Int* **58**:2320–2330.

Address correspondence to: Dr. Koichi Tan-No, Department of Pharmacology, Faculty of Pharmaceutical Sciences, Tohoku Medical and Pharmaceutical University, 4-4-1 Komatsushima, Aoba-ku, Sendai, Miyagi 981-8558, Japan. E-mail: koichi@tohoku-mpu.ac.jp